20th Australasian Fluid Mechanics Conference
Perth, Australia
5-8 December 2016

Pulsatile Flow Through a Compliant Channel: A Comparison of Laminar and Fully Developed Turbulent Flow Effects

K. Tsigklifis[1] **and A. D. Lucey** [1]

[1]Fluid Dynamics Research Group
Department of Mechanical Engineering
Curtin University,Perth, Westrn Australia 6845, Australia

Abstract

We investigate the fluid-structure interaction (FSI) of plane Poiseuille and fully developed turbulent flows through a compliant channel with flexible-plate-spring type walls. Although fundamental in nature, the study is partially motivated by its application to the biomechanics of blood flow. Our main objective is to assess the effect of modulation frequency and channel compliance on the wall shear stresses due to organized disturbances during the fundamental cycle of the unsteady mean flow. For the pulsatile plane Poiseuille mean flow an analytical solution is implemented, while the fully developed turbulent pulsatile mean flow is modelled via the unsteady RANS equations using the Boussinesq hypothesis for the Reynolds stresses. The eddy viscosity is calculated by solving the standard one-equation Spalart-Allmaras model. In order to compare the effects of the two types of mean flow on the FSI, we use the same bulk Reynolds number, the same dimensional applied pressure-gradient pulsation and the same dimensional properties for the compliant walls at each of a low ($Wo = 5$) and high ($Wo = 15$) modulation frequency (where Wo is the Womersely number). Our results show that even though the wall shear stresses of the turbulent pulsatile mean flow are larger than those of the laminar pulsatile mean flow within the pulsation cycle, the wall shear stresses induced by the organized disturbances are larger in the case of the laminar mean flow. Finally, wall compliance is shown to reduce the wall shear stresses due to the organized disturbances in all cases but this effect is more pronounced for the laminar mean flow at the low modulation frequency ($Wo = 5$).

Introduction

Biomechanical studies of the blood flow in arteries have shown that the magnitude of wall shear stress plays a significant role in both plaque formation and rupture. Laminar flow is thought to provide an atheroprotective role in mitigating localized elevation of the wall shear stresses [2, 3] that cause rupture. However, less is known about the effect of artery-wall compliance on the wall shear stresses induced by the mean pulsatile flow as well as by organised disturbances about the mean flow. Our very recent work [8] has systematically studied the stability of the pulsatile Poiseuille flow through a compliant channel revealing that the pulsatile flow is always stabilised by the existence of relatively stiff compliant walls for the entire range of modulation frequencies and dimensionless pressure-gradient modulation amplitudes in the range $\Lambda \leq 5$ and that this effect combines favourably with the stabilization effect of the Stokes layer. In the present paper, we extend this work to study the time-asymptotic and transient stability of a fully developed turbulent pulsatile channel flow with a focus on the size of the wall shear stresses generated by both the mean pulsatile flow and the organised disturbances during the modulation cycle. Our objective is to assess the effect of modulation frequency and wall compliance on the magnitudes of the mean and disturbance wall shear stresses and compare these values between laminar and fully developed turbulent pulsatile channel flows.

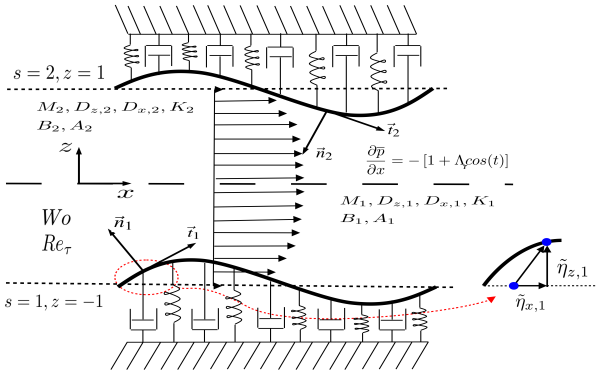

Figure 1: Schematic of the system studied

System Modelling

The formulation of the FSI problem that follows is based upon [8] in which laminar pulsatile mean flow supporting disturbances taking a spatial wave form was modelled; we now term these organised disturbances. When the pulsatile flow is turbulent, perturbations to the unsteady mean flow comprise both organised wave disturbances and turbulent fluctuations. It is the effect of the former that we study and therefore employ Reynolds averaged forms of the Navier-Stokes equations (RANS) wherein the turbulent Reynolds stresses contribute to both the determination of the mean flow and the evolution of the organised disturbances. With the laminar-flow case detailed in [8], we focus exclusively on the case of turbulent flow through the compliant channel.

Mean Turbulent Flow Field

We consider plane pulsatile viscous flow between two compliant walls separated by $2L^*$ distance as shown in figure 1. The characteristic length scale is chosen to be the half distance L^* between the (undisplaced) compliant surfaces, the velocity scale is the friction velocity, U^*_τ, of the underlying steady fully-developed turbulent flow about which pulsations occur, while the angular frequency of the applied periodic pulses defines the time scale, $1/\omega^*_f$. The flow field is then characterized by the Reynolds number based on the friction velocity, $Re_\tau = U^*_\tau L^*/\nu^*_l$, where ν^*_l is the kinematic viscosity of the fluid, and the Womersley number, $Wo = L^*(\omega^*_f/\nu^*_l)^{1/2}$. Here and hereafter, * denotes a dimensional quantity.

Following [6], we decompose the instantaneous velocity and pressure fields (becoming dimensionless through the dynamic pressure based on the friction velocity) as

$$u_i = \bar{u}_i + \tilde{u}_i + u'_i$$
$$p = \bar{p} + \tilde{p} + p', \qquad (1)$$

with $\bar{u}_i$ and $\bar{p}$ the mean velocity and pressure, u'_i and p' the turbulent velocity and pressure fluctuations, and $\tilde{u}_i$ and $\tilde{p}$ the velocity and pressure of the organised disturbances with prop-

erties $\overline{\tilde{p}} = \overline{p'} = \overline{\tilde{u}_i} = \overline{u'_i} = 0$, $\partial\overline{u}_i/\partial x_i = \partial\tilde{u}_i/\partial x_i = \partial u'_i/\partial x_i = 0$. Then, the time average of the Navier–Stokes equations in dimensionless form are

$$\frac{Wo^2}{Re_\tau}\frac{\partial\overline{u}_i}{\partial t} + \overline{u}_j\frac{\partial\overline{u}_i}{\partial x_j} = -\frac{\partial\overline{p}}{\partial x_i} + \frac{1}{Re_\tau}\frac{\partial^2\overline{u}_i}{\partial x_j\partial x_j} - \frac{\partial(\overline{u'_i u'_j})}{\partial x_j}, \qquad (2)$$

where it has been assumed that $|\tilde{u}_i\tilde{u}_j| \ll |u'_i u'_j|$, thus $\overline{\tilde{u}_i\tilde{u}_j} \approx 0$.

The closure problem for the Reynolds stresses in equation (2) is modeled via the isotropic eddy-viscosity model:

$$-\overline{u'_i u'_j} = \frac{G}{Re_\tau}\left(\frac{\partial\overline{u}_i}{\partial x_j} + \frac{\partial\overline{u}_j}{\partial x_i}\right), \qquad (3)$$

with $G = \nu^*_\tau/\nu^*_l$ being the dimensionless kinematic eddy viscosity.

In the two-dimensional system as notated in figure 1, $x_1 = x$, $x_2 = z$, $u_1 = u_x$ and $u_2 = u_z$, the mean flow is entirely in the streamwise direction x due to a mean pressure gradient in this direction and this is changed periodically with a frequency ω^*_f and amplitude Λ_T following

$$\frac{\partial\overline{p}}{\partial x} = \left.\frac{\mathrm{d}\overline{p}}{\mathrm{d}x}\right|_{st.}\left[1 + \Lambda_T\frac{exp(it) + exp(-it)}{2}\right], \quad \left.\frac{\mathrm{d}\overline{p}}{\mathrm{d}x}\right|_{st.} = -1. \qquad (4)$$

Upon application of equation (3) in equation (2) and assuming that the streamwise derivatives of the Reynolds stresses due to turbulent fluctuations are small compared with their cross-stream counterparts, we obtain the equation that determines the mean turbulent pulsatile channel flow,

$$\frac{Wo^2}{Re_\tau}\frac{\partial\overline{u}_x}{\partial t} = -\frac{\partial\overline{p}}{\partial x} + \frac{1}{Re_\tau}\frac{\partial^2\overline{u}_x}{\partial z^2} + \frac{G}{Re_\tau}\frac{\partial^2\overline{u}_x}{\partial z^2} + \frac{1}{Re_\tau}\frac{\partial G}{\partial z}\frac{\partial\overline{u}_x}{\partial z}, \qquad (5)$$

with the no-slip condition, $\overline{u}_x = 0$, on the walls. The dimensionless kinematic eddy viscosity $G = Xf_{u1}$, $f_{u1} = X^3/(X^3 + c^3_{u1})$, $c_{u1} = 7.1$, is modelled via the "standard" one equation of Spalart-Allmaras [7], which is written for the fully developed pulsatile channel flow in dimensionless form as

$$\frac{Wo^2}{Re_\tau}\frac{\partial X}{\partial t} + \overline{u}_x\frac{\partial X}{\partial x} = \frac{Wo^2}{Re_\tau}C_{b1}(1-f_{t2})SX - \frac{1}{Re_\tau}\left[C_{w1}f_w - \frac{C_{b1}}{\kappa^2}f_{t2}\right]\left(\frac{X}{d}\right)^2 + \frac{1}{\sigma Re_\tau}\left[\frac{\partial\left[(1+X)\frac{\partial X}{\partial x}\right]}{\partial x} + \frac{\partial\left[(1+X)\frac{\partial X}{\partial z}\right]}{\partial z}\right] + \frac{C_{b2}}{\sigma Re_\tau}\left[\left(\frac{\partial X}{\partial x}\right)^2 + \left(\frac{\partial X}{\partial z}\right)^2\right], \qquad (6)$$

where $S = \overline{\Omega} + (f_{u2}/(Wo^2\kappa^2 d^2))X$, $\overline{\Omega} = (Re_\tau/Wo^2)\sqrt{2\overline{\omega}_{ij}\overline{\omega}_{ij}}$, $\overline{\omega}_{ij} = (1/2)(\partial\overline{u}_i/\partial x_j - \partial\overline{u}_j/\partial x_i)$, d is the dimensionless distance from the field point to the nearest wall while f_{u2}, κ, f_w, C_{b1}, C_{b2}, f_{t2}, C_{w1} and σ are functions of X or constants given in [7].

Field of Organised Disturbances

We proceed by using the decomposition of (1) in the Navier-Stokes equations and applying ensemble averaging, taking into account that $\langle u_i\rangle = \overline{u}_i + \tilde{u}_i$ and $\langle p\rangle = \overline{p} + \tilde{p}$, to obtain

$$\frac{Wo^2}{Re_\tau}\frac{\partial\langle u_i\rangle}{\partial t} + \langle u_j\rangle\frac{\partial\langle u_i\rangle}{\partial x_j} = -\frac{\partial\langle p\rangle}{\partial x_i} + \frac{1}{Re_\tau}\frac{\partial^2\langle u_i\rangle}{\partial x_j\partial x_j} - \frac{\partial(\langle u'_i u'_j\rangle)}{\partial x_j}. \qquad (7)$$

Subtracting (2) from (7) we obtain the equation for the organised disturbances,

$$\frac{Wo^2}{Re_\tau}\frac{\partial\tilde{u}_i}{\partial t} + \overline{u}_j\frac{\partial\tilde{u}_i}{\partial x_j} + \tilde{u}_j\frac{\partial\overline{u}_i}{\partial x_j} = -\frac{\partial\tilde{p}}{\partial x_i} + \frac{1}{Re_\tau}\frac{\partial^2\tilde{u}_i}{\partial x_j\partial x_j} + \frac{\partial\tilde{r}_{ij}}{\partial x_j}, \qquad (8)$$

where $\tilde{r}_{ij} = -(\langle u'_i u'_j\rangle - \overline{u'_i u'_j})$ is the effect of the turbulent Reynolds stresses on the evolution of the organised disturbances and is of order $\tilde{r}_{ij} \sim O(\tilde{u}_i)$. The closure problem for $\tilde{r}_{ij}$ in equation (8) is modeled via the isotropic eddy-viscosity model that is similar to equation (3):

$$\tilde{r}_{ij} = \frac{G}{Re_\tau}\left(\frac{\partial\tilde{u}_i}{\partial x_j} + \frac{\partial\tilde{u}_j}{\partial x_i}\right), \qquad (9)$$

with G, calculated via equation (6).

Considering only two-dimensional organised disturbances and that the mean flow only has a velocity component in the streamwise direction, the final system of equations for the organised disturbances of the turbulent pulsatile channel flow is written as

$$\frac{\partial\tilde{u}_x}{\partial x} + \frac{\partial\tilde{u}_z}{\partial z} = 0$$
$$\frac{Wo^2}{Re_\tau}\frac{\partial\tilde{u}_x}{\partial t} + \overline{u}_x\frac{\partial\tilde{u}_x}{\partial x} + \tilde{u}_z\frac{\partial\overline{u}_x}{\partial z} = -\frac{\partial\tilde{p}}{\partial x} + \frac{1}{Re_\tau}\left(\frac{\partial^2\tilde{u}_x}{\partial x^2} + \frac{\partial^2\tilde{u}_x}{\partial z^2}\right) + \frac{\partial\tilde{r}_{xz}}{\partial z}$$
$$\frac{Wo^2}{Re_\tau}\frac{\partial\tilde{u}_z}{\partial t} + \overline{u}_x\frac{\partial\tilde{u}_z}{\partial x} = -\frac{\partial\tilde{p}}{\partial z} + \frac{1}{Re_\tau}\left(\frac{\partial^2\tilde{u}_z}{\partial x^2} + \frac{\partial^2\tilde{u}_z}{\partial z^2}\right) + \frac{\partial\tilde{r}_{zx}}{\partial x}, \qquad (10)$$

having only retained the dominant term $\tilde{r}_{xz}$ [9]. We now assume that the field of the organised disturbances takes the following spatial waveforms,

$$\tilde{u}_i(x,z,t) = \hat{u}_i(z,t)exp(i\alpha x) + \text{c.c.}$$
$$\tilde{p}(x,z,t) = \hat{p}(z,t)exp(i\alpha x) + \text{c.c.}, \qquad (11)$$

and substitute these in equations (10). We then eliminate the pressure disturbance amplitude, $\hat{p}(z,t)$, to give the evolution equation for organised disturbance as

$$Wo^2\frac{\partial}{\partial t}\mathcal{L}\hat{u}_z = (\mathcal{L} - i\alpha Re_\tau\overline{u}_x)\mathcal{L}\hat{u}_z + i\alpha Re_\tau\frac{\partial^2\overline{u}_x}{\partial z^2}\hat{u}_z + GQ^2\hat{u}_z + \frac{\partial^2 G}{\partial z^2}Q\hat{u}_z + 2\frac{\partial G}{\partial z}Q\frac{\partial\hat{u}_z}{\partial z}, \qquad (12)$$

where $\mathcal{L} = \partial^2/\partial z^2 - \alpha^2$, $Q = \partial^2/\partial z^2 + \alpha^2$.

Using equations (10), (11) and the continuity equation, we can express the pressure disturbance amplitude $\hat{p}(z,t)$ as the following function of $\hat{u}_z(z,t)$,

$$\hat{p} = -\frac{Wo^2}{\alpha^2 Re_\tau}\frac{\partial^2\hat{u}_z}{\partial t\partial z} - \frac{i\overline{u}_x}{\alpha}\frac{\partial\hat{u}_z}{\partial z} + \frac{i}{\alpha}\frac{\partial\overline{u}_x}{\partial z}\hat{u}_z + \frac{1}{\alpha^2 Re_\tau}\mathcal{L}\frac{\partial\hat{u}_z}{\partial z} + \frac{G}{\alpha^2 Re_\tau}Q\frac{\partial\hat{u}_z}{\partial z} + \frac{1}{\alpha^2 Re_\tau}\frac{\partial G}{\partial z}Q\hat{u}_z. \qquad (13)$$

For the compliant-wall dynamics, we use the one-dimensional isotropic Kirchhoff plate equation with additional terms to account for a dashpot-type damping and a uniformly distributed spring foundation. Combined with the normal and tangential force balance on the compliant walls, we obtain two equations which relate the vertical and axial displacements of the two compliant surfaces, $\tilde{\eta}_{z,s}(x,t)$ and $\tilde{\eta}_{x,s}(x,t)$ (for $s = 1,2$ lower/upper surfaces), with the pressure disturbance $\tilde{p}(x, z = \mp 1, t)$ and the velocity gradients of the mean and organised disturbances on the two interfaces (see [8]). The system of equations is completed with the enforcement of continuity of both the tangential and vertical disturbance velocities between fluid and solid [8], while the effect of turbulent velocity and pressure fluctuations at the interfaces are assumed negligible because their time-average is zero.

For spatial discretization in the direction normal to the mean flow, z, we use the Chebyshev pseudospectral method. The domain is discretized into $M+1$ collocation points and the spatial derivatives of a function at the these points are related to the values of the function through the Chebyshev differentiation matrices [1].

Solution Methodology

Equations (5) and (6) which describe the mean pulsatile flow are solved in space with the use of a second-order finite-difference scheme for the streamwise direction and the Chebyshev pseudospectral method for the direction perpendicular to the mean flow with periodic inlet-outlet boundary conditions. Both equations are solved using a second-order backward-difference time-stepping scheme using the following iterative algorithm: the linear equation (5) is solved for the mean velocity profile for given dimensionless kinematic eddy viscosity G from the previous time-step or iteration. The non-linear equation (6) is then solved for the eddy viscosity G using the quasi-Newton method by approximating the Jacobian through a first-order Euler scheme and the whole procedure is repeated until convergence of both the mean velocity profile and the eddy viscosity G are achieved after which the whole solution is advanced in time.

Concomitant with the decomposition of (1) we write the vertical and horizonal components of the complaint-wall deformations as $\tilde{\eta}_{z,s}(x,t) = \hat{\eta}_{z,s}(t)exp(\mathrm{i}\alpha x) + \text{c.c.}$ and $\tilde{\eta}_{x,s}(x,t) = \hat{\eta}_{x,s}(t)exp(\mathrm{i}\alpha x) + \text{c.c.}$ in the normal and tangential force balances of the compliant walls (see [8] for details). These are then used with equation (13), the continuity equation and the system of equations (12) with the two kinematic interfacial boundary conditions at each compliant surface, to cast in the following initial-value problem for the FSI system,

$$\frac{d\vec{\hat{v}}}{dt} = \underline{\underline{Q}}(t)\vec{\hat{v}},\ \vec{\hat{v}} = \{\hat{c}_{z,s}, \hat{\eta}_{z,s}, \hat{c}_{x,s}, \hat{\eta}_{x,s}, \vec{\hat{u}}_z^T\}^T,\ \vec{\hat{v}}(t=0) = \vec{\hat{v}}^0, \quad (14)$$

where $\hat{c}_{z,s} = \mathrm{d}\hat{\eta}_{z,s}/\mathrm{d}t$, $\hat{c}_{x,s} = \mathrm{d}\hat{\eta}_{x,s}/\mathrm{d}t$ and $\underline{\underline{Q}}$ is periodic in time with fundamental period T, due to the imposed periodic mean velocity $\overline{u}_x$.

The time-asymptotic stability of the system expressed by equation (14) can be studied through the eigenvalues of the monodromy matrix $\underline{\underline{M}}$. This is calculated by solving the following initial-value matrix problem [4]:

$$\underline{\underline{M}} = \underline{\underline{S}}(t=T): \quad \frac{d\underline{\underline{S}}}{dt} = \underline{\underline{Q}}(t)\underline{\underline{S}} \quad , \quad \underline{\underline{S}}(t=0) = \underline{\underline{I}} \quad , \qquad (15)$$

where $\underline{\underline{I}}$ is the identity matrix. Using a second-order backward integration scheme for time, the matrix $\underline{\underline{M}}$ is evaluated at the end of one period T from the product of the matrices calculated in the previous time-steps [8]. Its eigenvalues, the Floquet multipliers, $k_j, j = 1, \cdots M+1$ determine the stability of the pulsatile channel flow over the compliant walls in the following manner: Pulsatile flow is stable if $|k_j| < 1$ for $j = 1, 2, \cdots M+1$ and unstable if $|k_j| > 1$ for some j [4]. Alternatively, the system of equations (14) can be integrated in time with an initial vector based on the second-order backward-difference scheme to monitor the transient and asymptotic response of the FSI system.

Results and Discussion

Mean Flow Field

The mean pulsatile velocity profiles were validated through comparison with the results of [5]. The main purpose of the present work is to compare the wall shear stresses during the fundamental oscillation cycle produced by both the mean pulsatile flow and organized disturbances as generated by laminar and turbulent pulsatile mean velocity profiles for low ($Wo = 5$) and high ($Wo = 15$) modulation frequencies for identical dimensional flow conditions. The Reynolds number Re_b, based on the bulk velocity, and the dimensional pressure gradient modulation amplitude were selected to be those marginally above of the critical conditions (instability onset) for laminar pulsatile flow through a compliant channel with properties given in [8]. Specifically, for the given dimensional properties of the compliant walls, modulation frequency $Wo = 5$ and dimensionless amplitude of the pressure-gradient modulation $\Lambda = 3$ (made dimensionless through the centreline velocity of the corresponding steady flow; i.e. $\Lambda = 0$), the critical Reynolds number based on the centreline velocity of the steady flow is $Re_0 = 3775$; this produces a critical $Re_b = 2/3Re_0 = 2517$ or $Re_\tau = 161$. Using the same dimensional amplitude of the pressure-gradient modulation, its non-dimensional value for steady fully-developed turbulent flow is $\Lambda_T = 3\Lambda Re_b/Re_\tau^2 = 0.872$ (made dimensionless through the friction velocity). Similar calculations for laminar-flow critical conditions when $Wo = 15$ and $\Lambda = 5$ give $Re_b = 4333$ or $Re_\tau = 260$ and the corresponding turbulent-flow value $\Lambda_T = 0.965$.

Figure 2 shows the velocity profiles of the pulsatile mean flow through the (rigid-walled) channel for laminar and fully developed turbulent flow during one cycle of the applied pulsation at each of low ($Wo = 5$) and high ($Wo = 15$) modulation frequency. For $Wo = 5$, the laminar profile features an inflexion point during the cycle that can give rise to an amplified organised disturbance. In contrast, the turbulent profiles and laminar profile at $Wo = 15$ do not feature an inflexion point and can be expected to be stable for the present choice of dimensional bulk-flow speed and amplitude of the pressure-gradient modulation. Figure 3 shows the corresponding time evolution of the wall shear stresses due the mean flows presented in figure 2, $\overline{\tau}_w(z=-1) = (1/Re_\tau)(\partial\overline{u}_x/\partial z|_{z=-1} + \partial\overline{u}_z/\partial x|_{z=-1})$ over four periods of the modulation. It is seen that both the average shear stresses and their amplitudes of oscillation are greater when the mean flow is turbulent; this is clearly to be expected given the higher velocity gradient at the wall as compared with the laminar flow. Finally, in both laminar and turbulent cases, the amplitudes of the oscillations are larger for the low-frequency modulation because the magnitudes of mean-velocity fluctuations are much lower at $Wo = 15$ as can be seen in figure 2.

Field of Organized Disturbances

In the present work, we are mainly interested in investigating the effect of the mean velocity profile on the stability of the FSI system and the wall shear stresses produced by the organised disturbances. For this reason we solve the Orr-Sommerfeld type equation (12) without the contribution of the turbulent terms on the stability problem. The time-asymptotic stability of the fully developed turbulent pulsatile channel flow, studied through the extraction of the eigenvalues of the Monodromy matrix $\underline{\underline{M}}$ via the Floquet multipliers, reveals that the flow is stable with respect to growth of organised wave-like disturbances at both low ($Wo = 5$) and high ($Wo = 15$) modulation frequencies for both rigid and the relatively stiff compliant-channel walls used herein. Figures 4(a) and (b) show the time evolution of the wall shear stresses due to the organised disturbances over four periods of the modulation for the laminar and the turbulent pulsatile mean flow respectively and for $Wo = 5$, while figure (c), shows the same variables for $Wo = 15$. These results were generated by integration of equation (14) with the same dimensional initial vector, $\vec{\hat{v}}^{0*}$.

Figures 4(a) and (b) show that the disturbance wall shear stresses are significantly larger, by almost four orders of magnitude, for the laminar as compared with the turbulent pulsatile

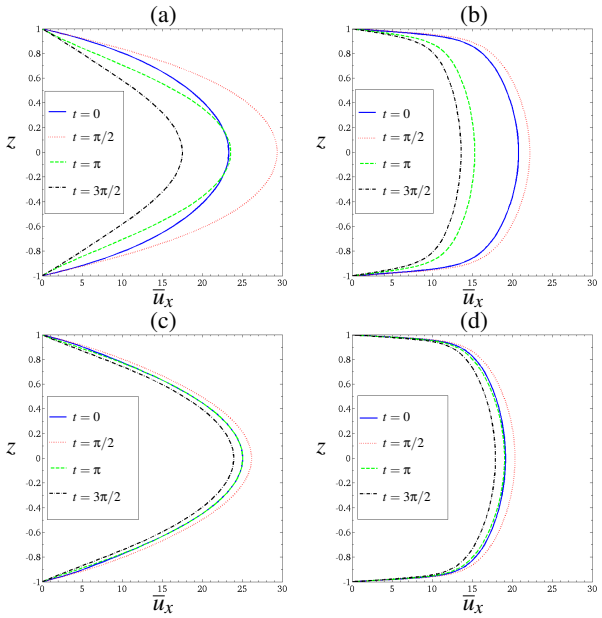

Figure 2: Velocity profiles during one cycle of the disturbance pressure gradient modulation for $Wo = 5$, $Re_\tau = 161$ for (a) pulsatile Poiseuille flow with $\Lambda = 3$, (b) fully developed turbulent pulsatile channel flow with $\Lambda_T = 0.872$. Velocity profiles for $Wo = 15$, $Re_\tau = 260$ for (c) pulsatile Poiseuille flow with $\Lambda = 5$, (d) fully developed turbulent pulsatile channel flow with $\Lambda_T = 0.965$.

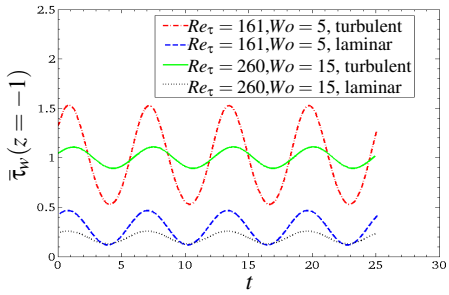

Figure 3: Time evolution of the mean wall shear stresses $\overline{\tau}_w$ of the bottom wall during four periods of the modulation, corresponding to the velocity profiles of figure 2.

mean flow. The effect of the wall-compliance is stabilising mainly for the laminar pulsatile flow as seen through both the time-asymptotic behaviour (details not shown here) and time-integrated initial-value problem that generated the data in figures 4(a) and (b) as evidenced by the reduction in amplitude of the fluctuating wall shear stresses in the laminar pulsatile flow. We also remark that the time-amplification of successive wave packets for the laminar-flow case reflects the fact that the organised disturbances are (marginally) unstable for the system parameters selected and discussed in the sub-section above. For high-frequency modulation, $Wo = 15$, the results of figure 4(c) show that the disturbance wall shear stresses produced by the laminar pulsatile flow are still larger than those of the turbulent pulsatile mean flow, while the compliant wall is much less effective in reducing the wall shear stresses in both cases; this might be expected because a relatively stiff compliant wall has been used in this preliminary investigation.

Conclusions

We have studied the time-asymptotic stability and compared the wall shear stresses generated by both the mean pulsatile channel flow and the organised disturbances for laminar and turbulent pulsatile flows through both rigid and flexible channels. Our results show that although the shear stresses due to the pulsatile

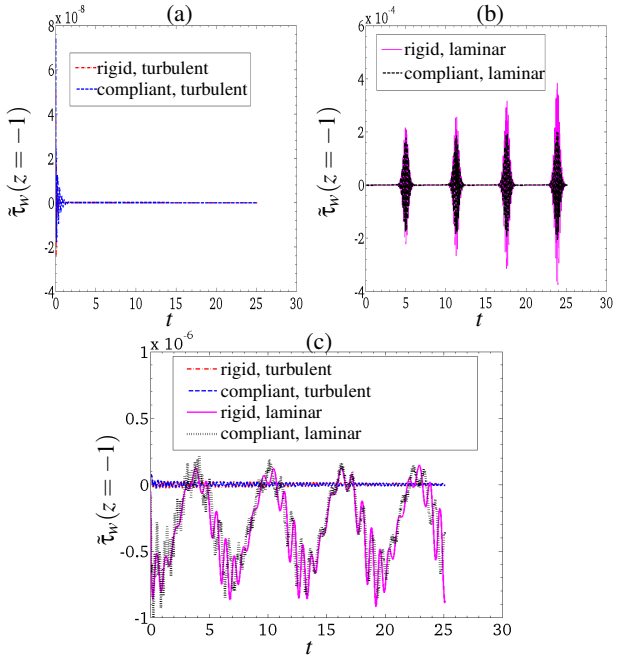

Figure 4: Time evolution of the wall shear stresses due to the organized disturbances for rigid and compliant channel flow for (a) and (b) $Wo = 5, Re_\tau = 161$, (c) $Wo = 15, Re_\tau = 260$

turbulent mean flow are larger than those of the equivalent laminar flow, the shear stresses due to organised wave-like disturbances are larger for the laminar flow. This is because inflectional velocity profiles occur during the deceleration phase of the modulation cycle in laminar flow; these are absent in the corresponding turbulent-flow profiles. Finally, wall-compliance has been shown to reduce disturbance wall shear stresses mainly for the laminar flow at low modulation frequency.

References

[1] Canuto, C., Hussaini, M.Y., Quarteroni, A. and Zang, T.A., *Methods in Fluid Dynamics*, Springer–Verlag, 1988.

[2] Cunningham, K.S. and Gotlieb, A.I., The Role of Shear Stress in the Pathogenesis of Atherosclerosis, *Laboratory Investigation*, **85**, 2005, 9–23.

[3] Fukumoto, Y., Hiro, T., Fujii, T., Hashimoto, G., Fujimura, T., Yamada, J., Okamura, T. and Matsuzaki, M., Localized Elevation of Shear Stress Is Related to Coronary Plaque Rupture , *Journal of the American College of Cardiology*, **51**, 6, 2008, 645–650.

[4] Iooss, G. and Joseph, D.D., *Elementary Stability and Bifurcation Theory*, Springer–Verlag New York, 1990.

[5] Scotti, A. and Piomelli, U., Turbulence Models in Pulsating Flows, *AIAA Journal*, **40**, 3, 2002, 537–544.

[6] Sen, P.K. and Veeravalli, S.V., On the Behaviour of Organised Disturbances in a Turbulent Boundary-Layer, *Sadhana*, **23**, 2, 1998, 167–193.

[7] Spalart, P.R. and Allmaras, S.R., A One-Equation Turbulence Model for Aerodynamic Flows, *Recherche Aerospatiale*, **1**, 1994, 5–21.

[8] Tsigklifis, K. and Lucey, A.D., The Stability of Plane Pulsatile Poiseuille Through a Compliant Channel, *11th International Conference on Flow–Induced Vibration*, 2016, The Hague, The Netherlands.

[9] Yeo, K.S., Zhao, H.Z. and Khoo, B.C., Turbulent boundary layer over a compliant surface: absolute and convective instabilities, *Journal of Fluid Mechanics*, **449**, 2001, 141–168.